HHS Public Access

Author manuscript

J Tissue Eng Regen Med. Author manuscript; available in PMC 2015 May 18.

Published in final edited form as:

J Tissue Eng Regen Med. 2013 July ; 7(7): 572–583. doi:10.1002/term.553.

CD45/CD11b Positive Subsets of Adult Lung Anchorage-Independent Cells Harness Epithelial Stem Cells

Yakov Peter[a,1], **Namita Sen**[1], **Elena Levantini**[b], **Steven Keller**[c], **Edward P Ingenito**[a], **Aaron Ciner**[1], **Robert Sackstein**[d], and **Steven D Shapiro**[e]

Yakov Peter: peter@yu.edu; Elena Levantini: elevanti@bidmc.harvard.edu; Steven Keller: skeller@montefiore.org; Edward P Ingenito: edward.ingenito@aerist.com; Robert Sackstein: rsackstein@rics.bwh.harvard.edu; Steven D Shapiro: sds33@pitt.edu

[a]Department of Pulmonary and Critical Care Medicine, Brigham and Women's Hospital and Harvard Medical School, Boston, MA 02115, USA

[b]Department of Hematology and Oncology, Beth Israel Deaconess Medical Center and Harvard Medical School, Boston, MA 02115, USA

[c]Department of Thoracic Surgery, Albert Einstein College of Medicine of Yeshiva University, Bronx, NY 10461, USA

[d]Department of Dermatology, Brigham and Women's Hospital and Harvard Medical School, Boston, MA 02115, USA

[e]Department of Medicine, University of Pittsburgh, Pittsburgh, PA 15261, USA

Abstract

Compensatory growth is mediated by multiple cell types that interact during organ repair. To elucidate the relationship between the stem/progenitor cells that proliferate or differentiate and the somatic cells of lung, we utilized a novel *ex vivo* pneumoexplant system. Applying this technique, we identified a sustained culture of repopulating adult progenitors in the form of free floating anchorage-independent cells (AICs). AICs did not express integrin proteins α5, β3, and β7, and constituted 37% of the total culture at day 14, yielding a mixed yet conserved population that recapitulated RNA expression patterns of the healthy lung. AICs exhibited rapid proliferation manifested by a marked 60-fold increase in cell numbers by day 21. Over 50% of the AIC population was $cKit^+$ or double-positive for $CD45^+$ and $CD11b^+$ antigenic determinants, consistent with cells of hematopoietic origin. The latter subset was found to be enriched with prosurfactant protein-C and SCGB1A1 expressing putative stem cells and with aquaporin-5 producing cells, characteristic of terminally differentiated alveolar epithelial type-1 pneumocytes.

Corresponding Author: Yakov Peter, PhD, Department of Biology, Yeshiva University, Belfer Hall #1406A, 500 W 185th St, New York, NY 10033. USA, Tel: (212) 960-5401, Fax: (212) 960-0035, yakov.peter@einstein.yu.edu, URL: http://www.einstein.yu.edu/home/faculty/profile.asp?id=11870&k=.

[1]**Permanent Address:**
Department of Biology and Pulmonary Medicine, Yeshiva University, New York, NY 10033.

Contributor Justification: YP - Conception and design, Collection and/or assembly of data, Data analysis and interpretation, Manuscript writing, Final approval of manuscript; NS, AC and EL - Collection and/or assembly of data; SK and EI - Provision of study material or patients; RS and SS – Data analysis and interpretation, financial support and manuscript review.

Author Disclosure Statement
No competing financial interests exist.

AICs undergo remodeling to form a cellular lining at the air/gel interface, and TGFβ1 treatment modifies protein expression, implying direct-differentiation of this population. These data confirm the active participation of clonogenic hematopietic stem cells in a mammalian model of lung repair and validate mixed stem/somatic cell cultures, which embrace sustained cell viability, proliferation, and differentiation, for use in studies of compensatory pulmonary growth.

Keywords

Anchorage-independent cells; Suspension culture; CD45/CD11b positive cells; Lung progenitors

1. Introduction

When cultivated on monolayer culture, cells from tissue explants are outgrown by, or behave morphologically and biochemically as rapidly proliferating fibroblasts (Coon 1966; Fehrenbach et al. 2009). In contrast, tissue cultivation on a semisolid culture has been shown to obstruct fibroblast overgrowth (Friedenstein et al. 1974; Torry et al. 1996; Bilko et al. 2005) to result in co-cultures of: 1) adherent stromal cells that may serve as feeder layers, and 2) non-attached, anchorage-independent cell (AIC) subsets (Rosenstraus et al. 1984; Borue et al. 2004). In the absence of adhesion proteins, AICs from marrow, liver, prostate, and adipose tissue have been reported to display clonogenic growth, form spheres, exhibit increased expression of putative stem cell markers, and multipotentially differentiate (Nemunaitis et al. 1989; Dalton et al. 1992; Jones et al. 1996; Lin et al. 2005; Shi et al. 2007; Lin and Chang 2008). Moreover, AIC growth in suspension required less extracellular growth promoting factors and were not restricted by cell-cell contacts (Shekhter-Levin et al. 1985; Arsic et al. 2008).

Pulmonary gas exchange takes place in the distal airways through a barrier of epithelial cells that line the airway with alveolar type (AT)-II cells secreting surfactant proteins and transdifferentiating into ATI cells (Chen et al. 2005; Qiao et al. 2008). It is known that an epithelial cell hierarchy exists in the lung with a class of progenitor cells staining positive for the surfactant protein C (pSPC) and secretoglobin, family 1A, member 1 (uteroglobin) (SCGB1A1) proteins. While the extracellular markers that characterize the pSPC/SCGB1A1 double positive cells remain controversial, several studies suggest a role for hematopoietic CD45 and the non-hematopoietic Sca-1 stem cell surface markers in lung regeneration with the CD45 (high) and CD11b (high) presenting leukocytes accumulating at sites of injury (Giangreco et al. 2004; Summer et al. 2004; Shim et al.). A dynamic *ex vivo* coculture system that cultivates stem and supporting cell subsets could thus recapitulate tissue homeostasis and compensatory growth (Weiss et al. 2006; Peter 2007; Blaisdell et al. 2009).

Many laboratories have attempted to determine alveolar signals and cell-proliferation with specially elaborated media and culture conditions (Gueven et al. 1996; Lang et al. 1998; Blickwede and Borlak 2005; Lang et al. 2007), as well as isolation techniques (Carley et al. 1992; Kim et al. 2005; Gonzalez et al. 2009) to study metabolism (Torky et al. 2005), transport (Demaio et al. 2009), and the potential of lung progenitors to drive repair (Bishop and Rippon 2006; Summer et al. 2007; Giangreco et al. 2009; McQualter et al. 2009). These

attempts have been at least partially thwarted by the fact that alveolar cell proliferation when grown in monolayers is regularly replaced by cell transdifferentiation (Chen et al. 2005; Qiao et al. 2008). To elucidate lung alveolar progenitor populations we focused on a newly described anchorage-independent cell population that can be maintained for long periods of time *in vitro*.

2. Materials and Methods

2.1. Mice and tissue sources

Male and female mice age 1–2 months (C57BL/6) were purchased from Charles River (Wilmington, MA), and green fluorescent protein (GFP) and β-galactosidase-expressing mice from Jackson laboratories (Bar Harbor, ME; #003115 and #002073, respectively). Sheep tissue was provided by E.I. at the Tufts Cummings School of Veterinary Medicine (Grafton, MA) and human tissue by S.K. at Montefiore Hospital (Bronx, NY). All experiments were performed according to protocols of the Harvard Medical Area and Yeshiva University Institutional Animal Care and Use Committees. Human studies were approved through the Committee on Clinical Investigations of Yeshiva University.

2.2. Pneumoexplant method

A 3.3% bactoagar gel (BD, Franklin Lakes, NJ) prepared from Dubelco's Modified Eagles Medium (DMEM; GIBCO, Grand Island, NY) + 10% bovine serum (Hyclone, Logan, UT) was prepoured (1 ml) into wells of a 12-well dish (Costar, Corning, NY) and allowed to set for one hour. This coating was submerged in 1 ml of the same composite growth medium (DMEM + serum). Lung tissue was carefully removed, rinsed in three successive plates of cold phosphate-buffered saline (PBS), finely chopped with microscissors, and two ~1 mm2 (weight = 35.1 ± 7.8 mg) tissue fragments were incubated in suspension at opposite poles of the well. PBS washes removed the majority of unbound (blood) cells prior to incubation, and the unprocessed lung was allowed to float in the upper layer of the well. Tissue fragments were removed from the dish on day 3 with fresh growth media added weekly (1:3 w/v). Cells were incubated at 37°C in a 5% CO_2 incubator (Thermo Scientific, Waltham, MA). This technique was modified from a previously described method to culture and differentiate granulocyte/macrophage hematopoietic progenitor cells in which bone marrow cells within the scaffold were replaced with lung fragments in the media layer (Peter et al. 2001).

2.3. Cell renewal and propagation experiments

AICs were collected, digested in 0.25% trypsin for 5 min. at 37°C, filtered through a strainer (70 micron, Corning, NY), diluted and single cells passaged by pipettation. Cell counts were performed in triplicates on individual wells of a 12-well dish at each time point. Total AIC numbers were calculated by the average number of cells/well multiplied by the number of wells prepared from a whole lung. Cell viability was determined by exclusion of the cell-impermeable dyes trypan blue and fluorescent propidium iodide (Sigma, St. Louis, MO), and the annexin V and 7-AAD containing, Nexin and Viacount dyes (Guava Technologies). Feeder layers were prepared from mouse embryonic day-14 mouse tail fibroblasts (MEFs) grown in DMEM, 10% fetal bovine serum (Hyclone), 1% nonessential amino acids, 1mM L-

glutamine, and 0.1 mM β-mercaptoethanol and irradiated at 40 Gy using a Gammacell 40 Exactor (Nordion International, Kanata, ON). For 5-Bromo-2'-deoxyuridine (BrdU) experiments, cells were treated with 10μg/ml BrdU (Sigma) for one hour, washed (×3 in PBS), permeabilized with 95% ethanol/ 5% acetic acid, washed (×3 in PBS) and stained. Differentiation into a honeycomb multicellular layer was performed by removal of the upper liquid media from two week-old AICs. Cells were maintained under a thin layer (100μl) of liquid growth media.

2.4. Immunofluorescence

Cells were cytocentrifuged onto slides, rinsed in cold PBS, fixed in 1% paraformaldehyde, stained with selected primary reagents, including goat or rabbit anti- secretoglobin, family 1A, member 1 (uteroglobin; SCGB1A1), rabbit anti-aquaporin 5 (Aqp5; Santa Cruz Biotech), rabbit anti-Ki67 (Abcam), and anti-prosurfactant protein C (pSPC; Millipore). Mouse anti-epidermal growth factor receptor, α smooth muscle actin, and BrdU were procured from Millipore, and mouse anti-actin and β-catenin were purchased from Sigma. Cells were then washed and treated with goat anti-mouse or chicken anti-goat Alexa-488 (Molecular Probes, Eugene,OR) or goat anti-rabbit Cyanine-3 (Jackson Immunoresearch Laboratories, West Grove, PA) secondaries, and covered with Fluoromount-G (Southern Biotech, Birmingham, AL). Following sorting, AICs were exposed to UV light for 10 minutes, and fluorescent quenching confirmed by microscopy.

2.5. Flow cytometry and sorting

Cells were dissociated in 0.13% trypsin for 10 minutes, washed and labeled with the following antibodies: PE-Cy5.5 or biotinylated rat anti-CD45R, PerCP-Cy5.5 conjugated anti-CD11b (ebioscience 12011283), R-PE conjugated rat-anti mouse Sca-1 (Invitrogen, Carlsbad, CA), APC conjugated anti-mouse cKit 17117183 (ebioscience, San Diego, CA), biotinylated anti-mouse CD31, TC conjugated anti-mouse CD45R (RM2606, Caltag, Burlingame, CA), Rabbit anti-EGFR (Cell signaling), streptavidin-PE/Cy5 and streptavidin-APC/Cy7 (Biolegend) and PE donkey anti-rabbit (Santa Cruz, CA) secondaries. Isotype controls included Alexa Fluor® 488 conjugated rat-IgG, FITC-rat IgG, R-PE-rabbit IgG (Southern Biotech, Birmingham, AL) and PE-Cy5.5 IgG (BD Pharmingen, San Diego, CA). To determine cell proliferation and apoptosis/necrosis we utilized the Click-iT 5- ethynyl-2'-deoxyuridine (EdU; Invitrogen, Carlsbad, CA) and Nexin (Merck, Whitehouse Station, NJ) assays, respectively. Experiments were performed per manufacturer's instructions. Briefly, AIC cells were pulsed with 10 μM EdU for 1 h. EdU-incorporated cells were fixed in paraformaldehyde for 15 min, permeabilized with a saponin-based buffer, and treated with the click-reaction mixture. Cells were analyzed on the Easycycle mini flow cytometer (Guava Technologies), FACScan (Becton Dickinson, Franklin Lakes, NJ), or MoFlo3 (Dako, Fort Collins, CO). Cytometric analysis was performed using the FlowJo software package (Ashland, OR).

2.6. Immunobloting

AICs were second round passaged (P2) onto 12-well dishes (Costar, Corning, NY) and treated with 2ng/ml of TGF-β1 (R&D systems, Minneapolis, MN) and refed three times weekly for a period of two weeks. Whole cell extracts were prepared in boiling sample

buffer (8% SDS, 0.2M Tris-HCl pH 6.8, 10mM EDTA, 40% glycerol) and supplemented with protease inhibitors (protease inhibitor cocktail, Sigma, St Louis, MO). Protein concentrations were determined (Bio-Rad DC Protein Assay, Hercules, CA) and 70 μg protein was loaded and electrophoresed in 10% SDS-polyacrylamide gels (Pierce, Rockford, IL), blotted onto nitrocellulose membranes (Bio-Rad, Hercules, CA), incubated with primary antibodies recognizing both human and mouse protein variants and detected by enhanced chemiluminescence (ECL; Amersham Biosciences, England). Secondary antibodies included horseradish peroxidase (HRP)-conjugated goat anti-mouse or goat anti-rabbit (Bio-Rad, Hercules, CA).

2.7. Nucleic acid purification, quantification, amplification, and RT of sample used for real-time qRT-PCR

RNA from total and sorted AICs was isolated from cells by the Trizol method (Invitrogen) and purified using RNeasy columns (Qiagen,Valencia, CA). RNA quality and quantity were determined by Nanodrop spectrophotometery (Thermo Scientific). First-strand cDNA synthesis using the SuperScript II reverse transcriptase kit (Invitrogen) was performed on 1mg total RNA using oligo(dT)12–18 (Invitrogen). To ensure an RT performance of equal quality, all samples were reverse transcribed simultaneously using a single mastermix. All reactions were performed in an ABI-PRISM 7300 sequence detection system (Applied Biosystems) starting with 10 min of *Taq* activation at 95°C, followed by 40 cycles of melting (95°C, 30 s), primer annealing at the temperature appropriate for each primer (55–60°C, 30s), and extension (72°C, 30s) ending with a melting curve analysis to validate the specificity of the PCR products. Fluorescence data were acquired after each annealing step. All primers were generated using the Primer3 software application and are listed in Supplementary Table 1. These include; Glyceraldehyde-3-phosphate dehydrogenase (*Gapdh*), CCAAT/enhancer binding protein alpha (*Cebpa*), *Scgb1a1*, pSPC (*Sftpc*), *Aqp5*, surfactant protein B (*Sftpb*), and CD31 (*Pecam1*). The absence of primer-dimers was verified post-amplification by melting curve analysis.

2.8. Cell scoring and signal quantification

AICs were sedimented by cytocentrifugation (Shandon, cytospin 4, Thermoscientific), labeled as indicated, immersed in fluorescent mounting medium and covered. The percentage of BrdU, alpha-smooth muscle actin, SCGB1A1, and pSPC expression to DAPI counterstained nuclear images were scored by two independent assessors blinded to treatment. Protein signal intensity was collected using Scion Image software application package (4.0.3.2, Scion Corporation, Frederick, MD) and normalized to that of β-actin.

2.9. Photographic capturing and statistical analysis

Photomicrographs were obtained using an Olympus IX71 microscope (Center Valley, PA) equipped with a DS-Qi1 camera head interfaced with NIS-Elements software (both from Nikon, Melville, NY). Images were globally adjusted for contrast and brightness and composed using Photoshop software (Adobe systems, San Jose, CA). Confocal images were captured using a T-3200 (Nikon Imaging Center, Harvard Medical School) or AOBS SP5 (Analytical Imaging Core, Albert Einstein College of Medicine) laser scanning microscopes.

Unless indicated, statistical analysis was performed using *F*-test for normally distributed data and Wilcoxon rank sum test for non-parametric skewed data. A significant difference between groups was established at $p<0.05$. Data are presented as average ± standard error of the mean (SEM).

3. Results and Discussion

Pneumoexplantation and AIC isolation from the lung

We developed a system where minced lung tissue was submersed in growth media and cultivated on a pre-poured soft-agar scaffold for three days. Cellular efflux from these tissue fragments resulted in either: 1) non-adherent cell growth in the liquid phase or; 2) adherent cell growth upon or within the scaffold (Supplementary Figure 1). Within mouse pneumoexplant bioreactors at day 14, the non-adherent AICs represented 37.0% ± 1.2% of the cultures with their percent viability demonstrated at 98.8% ± 2.3%, using trypan blue exclusion (data not shown). Finally, prior perfusion of the lung did not affect these results and AIC extraction and proliferation was validated in sheep and human pneumoexplant cultures (data not shown).

Next, to determine if AIC populations maintain characteristics of the lung, we compared by qRT-PCR the expression patterns of several lineage-specific mRNA transcripts (Table 1), specifically: *Sftpb* and *pSPC* (surfactant proteins produced by ATII cells), *Scgb1a1*(found in Clara cells), *Cebpa* (a transcription factor expressed in hematopoietic and ATII progenitors), aquaporin 5 (*Aqp5*; a water channel specific for ATI cells), and the endothelial cell marker *Pecam1* (Basseres et al. 2006). When normalized to the housekeeping gene, *Gapdh*, while transcript levels of *Cebpa*, *Aqp5*, and *Pecam1* were similar at day 7, production of *Sftpb*, *pSPC*, and *Scgb1a1* were reduced to approximately ~75% of normal lung expression. These differences were not statistically significant as determined by the non-parametric Wilcoxon test ($n\geq7$). These data indicate that AICs found in the lung are conserved throughout several organisms and can continue to reflect natural lung properties in culture.

AIC growth and proliferation in suspension culture

To reveal stem cell properties of AICs, we determined proliferative growth by plotting total number of cells in suspension at several time points (Figure 1A). While at day 1 post-explantation, an average of $8.8 \pm 0.4 \times 10^4$ AICs were recovered from the lung, by day 14 cell numbers leveled off at $5.5 \pm 1.6 \times 10^6$. These data represent a statistically significant 62-fold increase in cell numbers in two weeks ($n \geq 7$; $p = 6 \times 10^{-5}$). To validate cell proliferation we conducted flow cytometry and immunofluorescence labeling experiments at day 7, utilizing the incorporation of synthetic nucleotides EdU and BrdU, and labeling of anti-Ki67 antibodies that present nuclear proliferation in transitioning and dividing cells (Benayoun et al. 2001). Day 7 was chosen due to the larger number of identifiable cells in the bioreactor. As shown in Figure 1B, a shift in EdU staining was revealed in AICs with over 13% of the cells incorporating this nucleotide analogue. Similarly, both Ki67 nuclear localization and BrdU uptake was observed in separate experiments (Figure 1C and D), with BrdU incorporation observed in 15.8% ± 2.5% of the AIC population. By contrast, at day 24, only 0.4 ± 0.2% of cells demonstrated BrdU uptake, representing a significant decline in

proliferative growth over longer periods in culture ($n \geq 7$; $p<0.001$; data not shown). As seen in Figure 1E, dividing AICs did not express pSPC, reflecting either a separate proliferating lineage or a true undifferentiated phenotype known to define multipotential stem cells. Next, to quantify apoptosis and necrosis we utilized the annexin V reagent that binds phosphatidylserine on the outer surface of cells (associated with the onset of apoptosis) and the 7-AAD impermeable dye (an indicator of membrane structural integrity). Our data indicate apoptosis ranging between 0.5%–3.2% depending on reagents used, with no late apoptotic/necrotic cells found when gating for annexin V and 7-AAD fluorescence by flow cytometry (n=4; Figure 1F). These results indicate that AIC undergo a robust early proliferative-growth response that subsides over time in culture.

Clonogenic AIC growth on mouse embryonic feeder layers

To determine clonogenicity, we dissociated AICs from the lungs of GFP-expressing mice and reseeded single cells either on tissue culture plastic or mouse (wild-type) embryonic feeder layers (Supplementary Figure 2). Single cells passaged onto tissue culture plates resulted in limited proliferation that spread in a planar fashion on the dish. In contrast, seeding of single AICs on mouse embryonic feeder layers demonstrated perpendicular, substrate-independent, upgrowth resulting in the formation of cell colonies (defined as >50 cells). Over 2% of cells dissociated from these clones could maintain expansion when serially passaged and reseeded onto irradiated mouse embryonic fibroblast feeder layers. To further characterize AIC clones grown on MEFs, we determined the presence of the cKit stem cell marker, and pSPC and SCGB1A1 epithelial markers of the lower airways, by immunofluorescent microscopy (Supplementary Figure 2). cKit and pSPC demonstrated a punctate expression pattern while SCGB1A1 was detected in restricted areas within the clones. The reason for this discrepancy is unclear. Clonal expansion as well as the presence of stem cell and epithelial cell markers highlights the potential of AICs to differentiate into multiple cell types of the lung in culture.

Hematopoietic protein decoration of free floating AIC cultures

For classification and later as a metric for cellular changes/differentiation in culture, AIC antigen expression at days 6 and 21 was examined. As integrin subunits, which mediate cell attachment to the extracellular matrix, were shown to be deficient in anchorage independent cells (Dalton et al. 1999; Weinberg 2007), we tested by flow cytometry for the presence of integrin receptors on adult lung AICs and found a lack of integrins $\alpha 5$, $\beta 3$, and $\beta 7$ expression on both mouse and human populations (data not shown). In contrast, as shown in Table 2, integrin αM (CD11b) was greatly expressed in these cell types. Effectively, levels of CD11b increased in tandem with CD45 ($p \leq 0.05$) by day 21, concomitant with a significant reduction in the hematopoietic/lung stem cell marker, cKit ($p<0.001$). Moreover, the percentage of epidermal growth factor receptor (EGFR) and Pecam1 producing cells did not significantly change, indicating the presence of both epithelial and endothelial cells over time *in vitro*. Taken together, these data highlight presence of hematopoietic cell-associated markers that do not influence differentiated pulmonary cell types with time in culture.

Lung stem cells are enriched in the CD45/CD11b fraction

As CD45 and CD11b proteins were reported to be present on lung and airway progenitor cells, as well as on monocytic and hematopoietic subsets, we set out to determine the abundance of these markers in the AIC population (Rajantie et al. 2004; May et al. 2009). We found predominant expression of $CD45^+$ and $CD11b^+$ surface receptors within the AIC population with $CD45^+/CD11b^+$ double positive cells constituting approximately 60% of this fraction (Figures 2A–D). The stem cell marker Sca-1 and endothelial determinant CD31 were also highly represented in the AIC population (Figures 2E and 2F). To determine which of the above subsets might harbor lung pSPC/SCGB1A1 double positive cells, we applied fluorescent activated cell sorting and later subjected separated fractions to qRT-PCR and immunofluorescence. Surprisingly, while pSPC and Aqp5 proteins were identified by immunofluorescence following sorting, at the transcriptional level these mRNA's were diminished, indicating transcript instability (Table 1 and Figure 3). Cells of the $CD45^+/CD11b^+$ subset were found to produce Pecam1, Aqp5, the myofibroblastic cytoskeletal protein alpha-smooth muscle actin (αSMA) and, noteworthy, SCGB1A1 and pSPC proteins (Table 1 and Figure 3). In addition to the fact that SCGB1A1 and Aqp5 protein expression were explicitly found in the $CD45^+/CD11b^+$ subset, 26.0% ± 6.6% of this population was also shown to be double positive for pSPC and SCGB1A1 antigenic determinants, as revealed from immunofluorescent labeling ($n \geq 4$). These data indicate cell commitment towards epithelial lineages, as pSPC/SCGB1A1 double positive cells can delineate into both alveolar and terminal bronchial epithelial cell types. As SCGB1A1 was demonstrated in 65.3% ± 5.6% compared to pSPC that was found in 29.8% ± 10.2% of this cell population, preferential differentiation into the Clara lineage is predominant under these cellular conditions. In contrast, the $CD45^+/Sca\text{-}1^+$ subset was the most diverse with several statistically significant differences in transcript levels to AICs and $CD45^+/CD11b^+$ populations (Table 1). Taken together, these findings suggest the presence of a minor population of multipotential epithelial progenitor cells that reside within the $CD45^+/CD11b^+$ AIC subset.

Diverse AIC populations cooperate to form cell structures in vitro

To determine if AICs can undergo conditioned cell growth we exposed two week old cells to an air/gel interface, by significantly reducing the upper-suspension media interface. Under these conditions after two weeks, cells adhered to the scaffold and formed a polyhedral-structured multicellular layer that remained stable for an additional month (Figure 4A and 4B). To rule out cell clumping and to determine whether AICs can become polarized, we labeled multicellular day-21 layers for antibodies specific for the epidermal growth factor receptor (EGFR), reported to be predominantly localized at the apical membrane of ciliated lung epithelial cells (Tyner et al. 2006). EGFR labeling was chosen due to the length of time in culture and ordered cell structure that more likely represents a differentiated epithelial cell layer. In these experiments, EGFR was produced in AICs and localized at the cell periphery (Figure 4C), while actin stress fibers formed along neighboring cell membranes (data not shown) to imply establishment of cell polarization and functional contacts. Alternatively, cultivated for over a month, AICs could spontaneously align to form 3-dimensional cellular spheres in suspension (n=7; Figure 4D). We speculate that these structures form within air bubbles (spontaneous or induced) of the upper media layer. Taken together, continuous

interaction of mixed AIC layer subsets can promote cell remodeling and the generation of distinctive tissue-like structures in culture.

Activation of AIC subsets by transforming growth factor beta-1

To test the effect of soluble paracrine factors that induce cell transition or phenotypic changes primarily to epithelial cell populations, we removed two week old AICs and reseeded them in the absence or presence of 2ng/ml transforming growth factor beta-1 (TGFβ1). After a two week incubation period cells were then collected for immounoblotting (Figure 5). Untreated AICs were characterized by production of αSMA and lower amounts of pSPC, EGFR, and β-catenin proteins as compared to the A549 human lung epithelial cell line. As compared to non-treated AICs, TGFβ1 treatment elevated β-catenin that was accompanied by a decline in EGFR protein levels and pSPC levels. Measured by protein densitometry, subtracted by background and normalized to the housekeeping gene β-actin (data not shown; $n \geq 4$), changes in β-catenin and EGFR levels were statistically significant ($p < 0.05$). These results suggest that AIC subpopulations maintain the machinery to transduce TGFβ1 stimuli in culture and suggest that this immunosuppressive cytokine may promote AIC transition and/or differentiation.

The formidable challenges in understanding alveolar cell networks active during homeostasis and injury can be addressed using a multicellular pneumoexplant system to fractionate cells by their ability to bind a semisolid hydrogel. Applying this system, we expand on the reported lung cell populations and our data demonstrate that viable stem cells can be isolated from a population of adult anchorage-independent cells in a free-floating state from the lungs of several mammals. AICs represent a mixed population characterized by cKit expressing cells, as well as a CD45 and CD11b double positive fraction that harness pSPC and SCGB1A1 alveolar progenitor cells. Specifically, within this population, cells undergo clonogenic growth and are prone to phenotypic changes, while maintaining mRNA and protein expression in a pattern resembling that of the lung.

Our findings are consistent with prior reports that suggest that cKit is a marker for lung multipotential stem cells, and confirm the incidence of fibroblastic and epithelial lineages within cells of the AIC population (Horwitz and Dorfman 1970; Shin et al. 1975; Torry et al. 1996; Weinberg 2007; May et al. 2009; Kajstura et al. 2011). Furthermore, AIC proliferative growth recapitulates that of pluripotential colony-forming bone marrow and embryonic stem cells grown in suspension (Iscove and Yan 1990; zur Nieden et al. 2007), and convey plasticity when subjected to diverse environmental conditions or chemokines (Willis et al. 2005).

Presenting a hematopoietic cell phenotype, a major presence of CD45 and CD11b expressing cells in the AIC population may allude to the fact that: 1) the lung can function as a satellite organ of hematopoiesis to promote blood regeneration; 2) these cells can serve as a source of pulmonary cell precursors; and/or 3) these cells can support lung progenitor cells outside of the niche. These possibilities correspond with reports that identify CD45 and $CD45^{+}/CD11b^{+}$ expressing cells as epithelial and endothelial progenitors of the lung that together participate in postnatal vascular and airway repair and regeneration (Rajantie et al. 2004; Yamada and Takakura 2006; Zani et al. 2008; Li et al. 2009; May et al. 2009).

Recent influential studies have described the cKit receptor tyrosine kinase as a lung stem cell marker, with the reported cKit positive stem cells found localized to an unstructured niche of fibroblast, epithelial, smooth-muscle, and other cells (Kajstura et al. 2011; Lindsey et al. 2011). However, the conditions that drive derivation toward more specified $pSPC^{+}$/$SCGB1A1^{+}$ epithelial progenitors present in both $EpCAM^{hi}$ $CD49f^{+}$ $CD104^{+}$ $CD24^{low}$ and $CD45^{-}$ $CD31^{-}$ $Sca1^{+}$ $CD34^{+}$ populations remain elusive (Kim et al. 2005; McQualter et al. 2009; Raiser and Kim 2009). Clonogenic growth, accommodation of cKit expressing cells, that decrease with time in culture, as well as presence of the pSPC and SCGB1A1 lineage, highlights this strategy for stem cell isolation and may be further used to understand cues involved in stem cell derivation. Moreover, this technique may spare cells from mRNA instabilities and other artifacts associated with the absence of (stem cell) supporting cells or rigorous proteolytic tissue dissociation. These anomalies can be particularly misleading in attempts of stem cell identification (such as in the case of pSPC transcript degradation). Thus, cell characterization by mRNA and membranal protein attributes do not unequivocally determine classification and additional physiological factors, including the path of cell differentiation, chemokine activation, and/or attachment properties to a scaffold, may significantly assist in stem cell classification.

Cell proliferation, the presence of a comparable AIC transcript array, as well as a limited number of antigenic determinants suggest a similar cell ancestor, which serves in the pneumoexplant model as an early multipotential adult precursor. These cells may interact with their more determined progeny to maintain and coordinate compensatory growth with mesenchymal cells laying the (matrix) foundation upon which endothelial and epithelial populations can subsequently thrive. Of AIC populations, it is plausible that the $CD45^{+}$/$CD11b^{+}$ subset maintains an epithelial cell hierarchy as revealed by the prevalence of pSPC (ATII), SCGB1A1 (Clara), and Aqp5 (ATI) transcripts and proteins, as well as Cebpa found to be expressed in ATII progenitor cell types (Basseres et al. 2006). Cell conditioning at an air/gel interface leading to the formation of a cell lining with cuboidal morphology is reminiscent of secretive or absorptive tissue and could reflect the formation of distal bronchial epithelium. SCGB1A1, as well as epithelial-derived, epidermal growth factor receptor expression considerably bolsters this prospect. A more focused interrogation of the $CD45^{+}$/$CD11b^{+}$ subset, as well as their interactions with additional populations remains a subject for future AIC studies. Taken together, as the CD45 and CD11b double positive population exhibits robust expansion and harbors the reported $pSPC^{+}$/$SCGB1A1^{+}$ cells, which can be cultivated for up to three weeks in culture, these data support the use of the pneumoexplantation model as a system to study lung dynamics, and cell derivation and multi-cellular networks under stable and reproducible conditions.

These findings should be interpreted in the context of the study design. While in this model AICs are released into suspension it is possible that this observation may transpire from mechanical damage to the lung, specifically the application of coarse tissue mincing. In fact, *in vivo*, AICs may reside in the lung interstitium becoming motile following injury, translocating paracellularly to the lumenal (surfactant coated) surface of the lung, where conventional basement membrane and anchoring integrin subunits are absent. In this environment, AIC derivatives can exploit the lipid-rich media for: a) chemokine and growth

factor secretion; b) surfactant release; c) engulfment of dead tissue; and d) deposition of newly generated cells. Moreover, at this interface, distally located AICs could undergo unrestricted chemotaxis and mobilization to sites of alveolar injury. Such a mechanism is supported by the confinement of multiple growth factor receptors, including the EGFR, to the apical surface of lung epithelia and can explain why AICs are liberated solely by flooding tissue with growth media, in the absence of proteolytic enzyme requirements. Taken together, based upon our results we reason that AIC “mobile units” orchestrate regenerative lung growth from the airways, at sites of external pathogen or chemical assault.

We cannot confirm the exact lineage of AICs or rule out the possibility that cell explants undergo atypical differentiation following long-term cultivation. Hence, AIC expression patterns may not reflect that solely of the lung, with separate reports describing SFTPB and SCGB1A1 production in hematopoietic cells (Field-Corbett et al. 2009; Londhe et al. 2010). Along these lines, the fact that AICs expand in culture and cells of the CD45/CD11b fraction specifically express pSPC, SCGB1A1, and SFTPB proteins may indeed suggest a transient CD45/CD11b/pSPC/SCGB1A1 positive hematopoietic derivative that can participate in lung repair. This prospect corresponds with classical studies of normal mammalian lung cell proliferation that related dividing cells in the alveolar wall to alveolar macrophages and may now be used to explain the presence of the cKit hematopoietic stem cell marker as a determinant of human lung stem cells (Bertalanffy 1964; Kajstura et al. 2011; Lindsey et al. 2011). Finally, while we cannot exclude the option that pSPC/SCGB1A1 stem cells constitute contaminants that co-purify in the CD45/CD11b fraction, at the very least, this study provides evidence for the first time that CD45/CD11b cells interact with, and may support, endogenous lung progenitors for moderate periods of time in culture. Taken together, long-term mixed stem cell preservation by pneumoexplanation provides a significant advantage over contemporary methods employed to study cell derivation, interactions, and autonomic specification. Moreover, it is feasible that AICs, enriched for progenitor and spontaneously differentiated lung cells, might engage under these defined conditions in inductive interactions to promote cooperative growth. This type of development can potentially be applied to novel medical therapies with mixed-cell grafts replacing organ transplantation and serving as a viable alternative to transplantation of purified, lineage-restricted, stem cell populations. This exciting prospect remains an important topic for future studies.

In summary, the present study demonstrates a pneumoexplant culture to identify diverse populations that grow in suspension and emulate the natural cellular milieu of the lung. Employing this method, the versatile AIC population and its CD45/CD11b progenitor subset may help shed light on stem cell networks and circuits to elaborate on the minimal conditions necessary for compensatory lung growth.

Supplementary Material

Refer to Web version on PubMed Central for supplementary material.

Acknowledgments

The authors would like to thank Drs. Simon Spivack and Joseph Locker for their valuable comments; Maria Katherine Fernandez for human patient consent; Erica Tsacoyeanes, Sheli Hofmeister, and Batya Gounder for cell counts and measurements. * This work was supported by NIH grants HL 007633 (SDS), HL073714 (RS) and the Henry Kressel foundation (YP).

References

Arsic N, Mamaeva D, Lamb NJ, Fernandez A. Muscle-derived stem cells isolated as non-adherent population give rise to cardiac, skeletal muscle and neural lineages. Exp Cell Res. 2008; 314(6): 1266–1280. [PubMed: 18282570]

Basseres DS, Levantini E, Ji H, Monti S, Elf S, Dayaram T, Fenyus M, Kocher O, Golub T, Wong KK, et al. Respiratory failure due to differentiation arrest and expansion of alveolar cells following lung-specific loss of the transcription factor C/EBPalpha in mice. Mol Cell Biol. 2006; 26(3):1109–1123. [PubMed: 16428462]

Benayoun L, Letuve S, Druilhe A, Boczkowski J, Dombret MC, Mechighel P, Megret J, Leseche G, Aubier M, Pretolani M. Regulation of peroxisome proliferator-activated receptor gamma expression in human asthmatic airways: relationship with proliferation, apoptosis, and airway remodeling. Am J Respir Crit Care Med. 2001; 164(8 Pt 1):1487–1494. [PubMed: 11704601]

Bertalanffy FD. Respiratory tissue: structure, histophysiology, cytodynamics. II. New approaches and interpretations. Int Rev Cytol. 1964; 17:213–297. [PubMed: 5337624]

Bilko NM, Votyakova IA, Vasylovska SV, Bilko DI. Characterization of the interactions between stromal and haematopoietic progenitor cells in expansion cell culture models. Cell Biol Int. 2005; 29(1):83–86. [PubMed: 15763504]

Bishop AE, Rippon HJ. Stem cells--potential for repairing damaged lungs and growing human lungs for transplant. Expert Opin Biol Ther. 2006; 6(8):751–758. [PubMed: 16856797]

Blaisdell CJ, Gail DB, Nabel EG. Concise Review: NHLBI Perspective: Lung Progenitor and Stem Cells-Gaps in Knowledge and Future Opportunities. Stem Cells. 2009

Blickwede M, Borlak J. Isolation and characterization of metabolically competent pulmonary epithelial cells from pig lung tissue. Xenobiotica. 2005; 35(10–11):927–941. [PubMed: 16393853]

Borue X, Lee S, Grove J, Herzog EL, Harris R, Diflo T, Glusac E, Hyman K, Theise ND, Krause DS. Bone marrow-derived cells contribute to epithelial engraftment during wound healing. American Journal of Pathology. 2004; 165(5):1767–1772. [PubMed: 15509544]

Carley WW, Niedbala MJ, Gerritsen ME. Isolation, cultivation, and partial characterization of microvascular endothelium derived from human lung. Am J Respir Cell Mol Biol. 1992; 7(6):620–630. [PubMed: 1333246]

Chen SP, Zhou B, Willis BC, Sandoval AJ, Liebler JM, Kim KJ, Ann DK, Crandall ED, Borok Z. Effects of transdifferentiation and EGF on claudin isoform expression in alveolar epithelial cells. J Appl Physiol. 2005; 98(1):322–328. [PubMed: 15361518]

Coon HG. Clonal stability and phenotypic expression of chick cartilage cells in vitro. Proc Natl Acad Sci U S A. 1966; 55(1):66–73. [PubMed: 5328643]

Dalton SL, Marcantonio EE, Assoian RK. Cell attachment controls fibronectin and alpha 5 beta 1 integrin levels in fibroblasts. Implications for anchorage-dependent and -independent growth. J Biol Chem. 1992; 267(12):8186–8191. [PubMed: 1373721]

Dalton SL, Scharf E, Davey G, Assoian RK. Transforming growth factor-beta overrides the adhesion requirement for surface expression of alpha(5)beta(1) integrin in normal rat kidney fibroblasts. A necessary effect for induction of anchorage-independent growth. J Biol Chem. 1999; 274(42): 30139–30145. [PubMed: 10514503]

Demaio L, Tseng W, Balverde Z, Alvarez JR, Kim KJ, Kelley DG, Senior RM, Crandall ED, Borok Z. Characterization of mouse alveolar epithelial cell monolayers. Am J Physiol Lung Cell Mol Physiol. 2009; 296(6):L1051–L1058. [PubMed: 19329539]

Fehrenbach ML, Cao G, Williams JT, Finklestein JM, Delisser HM. Isolation of murine lung endothelial cells. Am J Physiol Lung Cell Mol Physiol. 2009; 296(6):L1096–L1103. [PubMed: 19304908]

Field-Corbett C, English K, O'Dea S. Regulation of surfactant protein B gene expression in bone marrow-derived cells. Stem Cells. 2009; 27(3):662–669. [PubMed: 19096034]

Friedenstein AJ, Deriglasova UF, Kulagina NN, Panasuk AF, Rudakowa SF, Luria EA, Ruadkow IA. Precursors for fibroblasts in different populations of hematopoietic cells as detected by the in vitro colony assay method. Exp Hematol. 1974; 2(2):83–92. [PubMed: 4455512]

Giangreco A, Arwert EN, Rosewell IR, Snyder J, Watt FM, Stripp BR. Stem cells are dispensable for lung homeostasis but restore airways after injury. Proc Natl Acad Sci U S A. 2009; 106(23):9286–9291. [PubMed: 19478060]

Giangreco A, Shen H, Reynolds SD, Stripp BR. Molecular phenotype of airway side population cells. Am J Physiol Lung Cell Mol Physiol. 2004; 286(4):L624–L630. [PubMed: 12909587]

Gonzalez RF, Allen L, Dobbs LG. Rat alveolar type I cells proliferate, express OCT-4, and exhibit phenotypic plasticity in vitro. Am J Physiol Lung Cell Mol Physiol. 2009

Gueven N, Glatthaar B, Manke HG, Haemmerle H. Co-cultivation of rat pneumocytes and bovine endothelial cells on a liquid-air interface. Eur Respir J. 1996; 9(5):968–975. [PubMed: 8793459]

Horwitz AL, Dorfman A. The growth of cartilage cells in soft agar and liquid suspension. J Cell Biol. 1970; 45(2):434–438. [PubMed: 4935443]

Iscove NN, Yan XQ. Precursors (pre-CFCmulti) of multilineage hemopoietic colony-forming cells quantitated in vitro. Uniqueness of IL-1 requirement, partial separation from pluripotential colony-forming cells, and correlation with long term reconstituting cells in vivo. J Immunol. 1990; 145(1): 190–195. [PubMed: 2358672]

Jones J, Sugiyama M, Speight PM, Watt FM. Restoration of alpha v beta 5 integrin expression in neoplastic keratinocytes results in increased capacity for terminal differentiation and suppression of anchorage-independent growth. Oncogene. 1996; 12(1):119–126. [PubMed: 8552382]

Kajstura J, Rota M, Hall SR, Hosoda T, D'Amario D, Sanada F, Zheng H, Ogorek B, Rondon-Clavo C, Ferreira-Martins J, et al. Evidence for human lung stem cells. N Engl J Med. 2011; 364(19):1795–1806. [PubMed: 21561345]

Kim CF, Jackson EL, Woolfenden AE, Lawrence S, Babar I, Vogel S, Crowley D, Bronson RT, Jacks T. Identification of bronchioalveolar stem cells in normal lung and lung cancer. Cell. 2005; 121(6):823–835. [PubMed: 15960971]

Lang DS, Droemann D, Schultz H, Branscheid D, Martin C, Ressmeyer AR, Zabel P, Vollmer E, Goldmann T. A novel human ex vivo model for the analysis of molecular events during lung cancer chemotherapy. Respir Res. 2007; 8:43. [PubMed: 17567922]

Lang DS, Jorres RA, Mucke M, Siegfried W, Magnussen H. Interactions between human bronchoepithelial cells and lung fibroblasts after ozone exposure in vitro. Toxicol Lett. 1998; 96–97:13–24.

Li B, Bailey AS, Jiang S, Liu B, Goldman DC, Fleming WH. Endothelial cells mediate the regeneration of hematopoietic stem cells. Stem Cell Res. 2009

Lin RZ, Chang HY. Recent advances in three-dimensional multicellular spheroid culture for biomedical research. Biotechnol J. 2008; 3(9–10):1172–1184. [PubMed: 18566957]

Lin TM, Tsai JL, Lin SD, Lai CS, Chang CC. Accelerated growth and prolonged lifespan of adipose tissue-derived human mesenchymal stem cells in a medium using reduced calcium and antioxidants. Stem Cells Dev. 2005; 14(1):92–102. [PubMed: 15725748]

Lindsey JY, Ganguly K, Brass DM, Li Z, Potts EN, Degan S, Chen H, Brockway B, Abraham SN, Berndt A, et al. c-KIT is Essential for Alveolar Maintenance and Protection From Emphysema-Like Disease in Mice. Am J Respir Crit Care Med. 2011

Londhe VA, Maisonet TM, Lopez B, Jeng JM, Li C, Minoo P. A Subset of Epithelial Cells with CCSP-promoter Activity Participates in Alveolar Development. Am J Respir Cell Mol Biol. 2010

May LA, Kicic A, Rigby P, Heel K, Pullen TL, Crook M, Charles A, Banerjee B, Ravine D, Saxena A, et al. Cells of epithelial lineage are present in blood, engraft the bronchial epithelium, and are increased in human lung transplantation. J Heart Lung Transplant. 2009; 28(6):550–557. [PubMed: 19481014]

McQualter JL, Brouard N, Williams B, Baird BN, Sims-Lucas S, Yuen K, Nilsson SK, Simmons PJ, Bertoncello I. Endogenous fibroblastic progenitor cells in the adult mouse lung are highly enriched in the sca-1 positive cell fraction. Stem Cells. 2009; 27(3):623–633. [PubMed: 19074419]

Nemunaitis J, Andrews DF, Mochizuki DY, Lilly MB, Singer JW. Human marrow stromal cells: response to interleukin-6 (IL-6) and control of IL-6 expression. Blood. 1989; 74(6):1929–1935. [PubMed: 2679911]

Peter Y. Tracheotomy: a method for transplantation of stem cells to the lung. J Vis Exp. 2007; (2):163. [PubMed: 18830428]

Peter Y, Rotman G, Lotem J, Elson A, Shiloh Y, Groner Y. Elevated Cu/Zn-SOD exacerbates radiation sensitivity and hematopoietic abnormalities of Atm-deficient mice. EMBO J. 2001; 20(7):1538–1546. [PubMed: 11285218]

Qiao R, Yan W, Clavijo C, Mehrian-Shai R, Zhong Q, Kim KJ, Ann D, Crandall ED, Borok Z. Effects of KGF on alveolar epithelial cell transdifferentiation are mediated by JNK signaling. Am J Respir Cell Mol Biol. 2008; 38(2):239–246. [PubMed: 17872496]

Raiser DM, Kim CF. Commentary: Sca-1 and Cells of the Lung: A matter of Different Sorts. Stem Cells. 2009; 27(3):606–611. [PubMed: 19259938]

Rajantie I, Ilmonen M, Alminaite A, Ozerdem U, Alitalo K, Salven P. Adult bone marrow-derived cells recruited during angiogenesis comprise precursors for periendothelial vascular mural cells. Blood. 2004; 104(7):2084–2086. [PubMed: 15191949]

Rosenstraus MJ, Sterman B, Carr A, Brand L. Fibroblast feeder layers inhibit differentiation of retinoic acid-treated embryonal carcinoma cells by increasing the probability of stem cell renewal. Exp Cell Res. 1984; 152(2):378–389. [PubMed: 6723794]

Shekhter-Levin S, Amato D, Karrass L, Axelrad AA. Heterogeneity of buoyant density and proliferative state of circulating erythropoietic progenitor cells (BFU-E) in man. Exp Hematol. 1985; 13(11):1138–1142. [PubMed: 4065262]

Shi X, Gipp J, Bushman W. Anchorage-independent culture maintains prostate stem cells. Dev Biol. 2007; 312(1):396–406. [PubMed: 17976567]

Shim YM, Paige M, Hanna H, Kim SH, Burdick MD, Strieter RM. Role of LTB in the pathogenesis of elastase-induced murine pulmonary emphysema. Am J Physiol Lung Cell Mol Physiol. 2010; 299(6):L749–L759. [PubMed: 20817777]

Shin SI, Freedman VH, Risser R, Pollack R. Tumorigenicity of virus-transformed cells in nude mice is correlated specifically with anchorage independent growth in vitro. Proc Natl Acad Sci U S A. 1975; 72(11):4435–4439. [PubMed: 172908]

Summer R, Fitzsimmons K, Dwyer D, Murphy J, Fine A. Isolation of an adult mouse lung mesenchymal progenitor cell population. Am J Respir Cell Mol Biol. 2007; 37(2):152–159. [PubMed: 17395889]

Summer R, Kotton DN, Sun X, Fitzsimmons K, Fine A. Translational physiology: origin and phenotype of lung side population cells. Am J Physiol Lung Cell Mol Physiol. 2004; 287(3):L477–L483. [PubMed: 15047566]

Torky AR, Stehfest E, Viehweger K, Taege C, Foth H. Immuno-histochemical detection of MRPs in human lung cells in culture. Toxicology. 2005; 207(3):437–450. [PubMed: 15664271]

Torry DJ, Richards CD, Podor TJ, Gauldie J. Modulation of the anchorage-independent phenotype of human lung fibroblasts obtained from fibrotic tissue following culture with retinoid and corticosteroid. Exp Lung Res. 1996; 22(2):231–244. [PubMed: 8706638]

Tyner JW, Kim EY, Ide K, Pelletier MR, Roswit WT, Morton JD, Battaile JT, Patel AC, Patterson GA, Castro M, et al. Blocking airway mucous cell metaplasia by inhibiting EGFR antiapoptosis and IL-13 transdifferentiation signals. J Clin Invest. 2006; 116(2):309–321. [PubMed: 16453019]

Weinberg, R. The Biology of Cancer. London: Garland Science; 2007.

Weiss DJ, Berberich MA, Borok Z, Gail DB, Kolls JK, Penland C, Prockop DJ. Adult stem cells, lung biology, and lung disease. NHLBI/Cystic Fibrosis Foundation Workshop. Proc Am Thorac Soc. 2006; 3(3):193–207. [PubMed: 16636086]

Willis BC, Liebler JM, Luby-Phelps K, Nicholson AG, Crandall ED, du Bois RM, Borok Z. Induction of epithelial-mesenchymal transition in alveolar epithelial cells by transforming growth factor-

beta1: potential role in idiopathic pulmonary fibrosis. Am J Pathol. 2005; 166(5):1321–1332. [PubMed: 15855634]

Yamada Y, Takakura N. Physiological pathway of differentiation of hematopoietic stem cell population into mural cells. J Exp Med. 2006; 203(4):1055–1065. [PubMed: 16606664]

Zani BG, Kojima K, Vacanti CA, Edelman ER. Tissue-engineered endothelial and epithelial implants differentially and synergistically regulate airway repair. Proc Natl Acad Sci U S A. 2008; 105(19): 7046–7051. [PubMed: 18458330]

zur Nieden NI, Cormier JT, Rancourt DE, Kallos MS. Embryonic stem cells remain highly pluripotent following long term expansion as aggregates in suspension bioreactors. J Biotechnol. 2007; 129(3):421–432. [PubMed: 17306403]

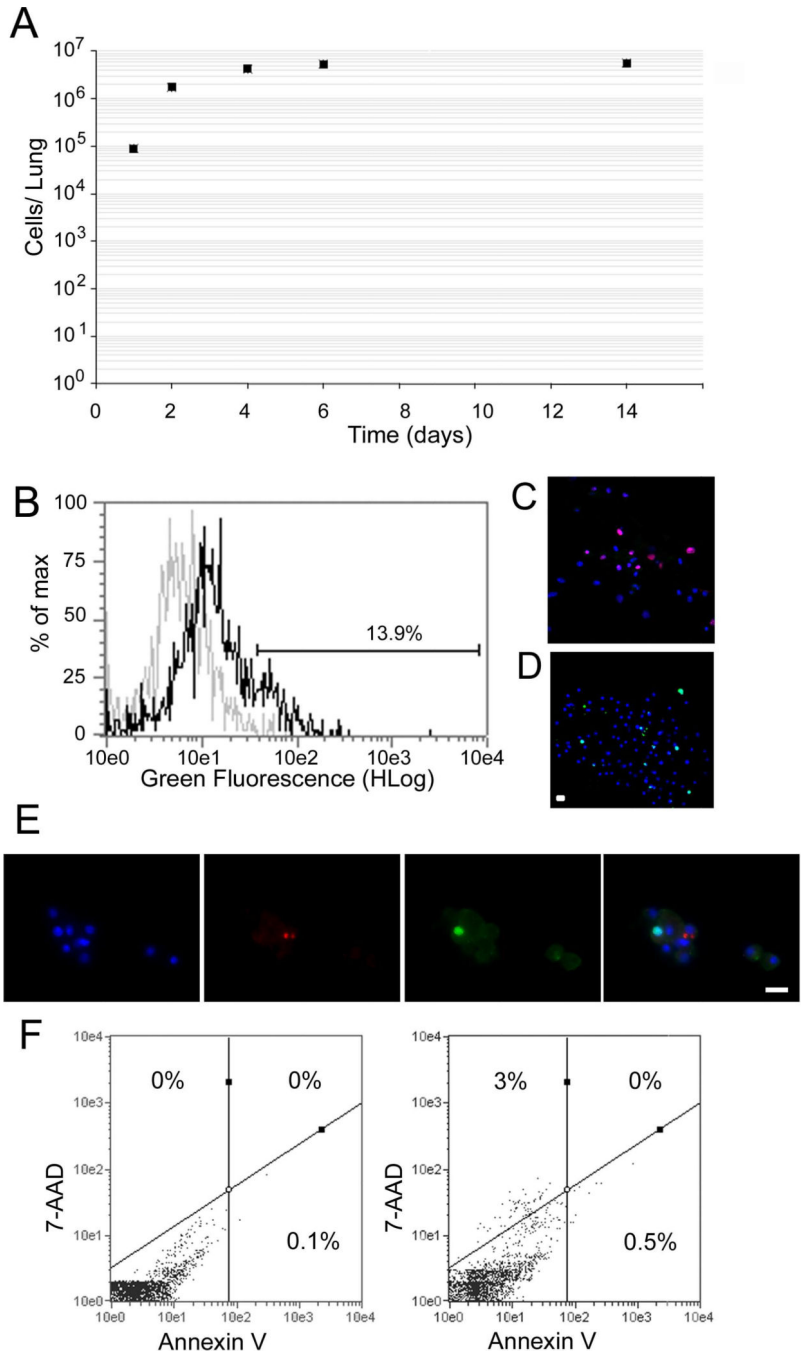

Figure 1.

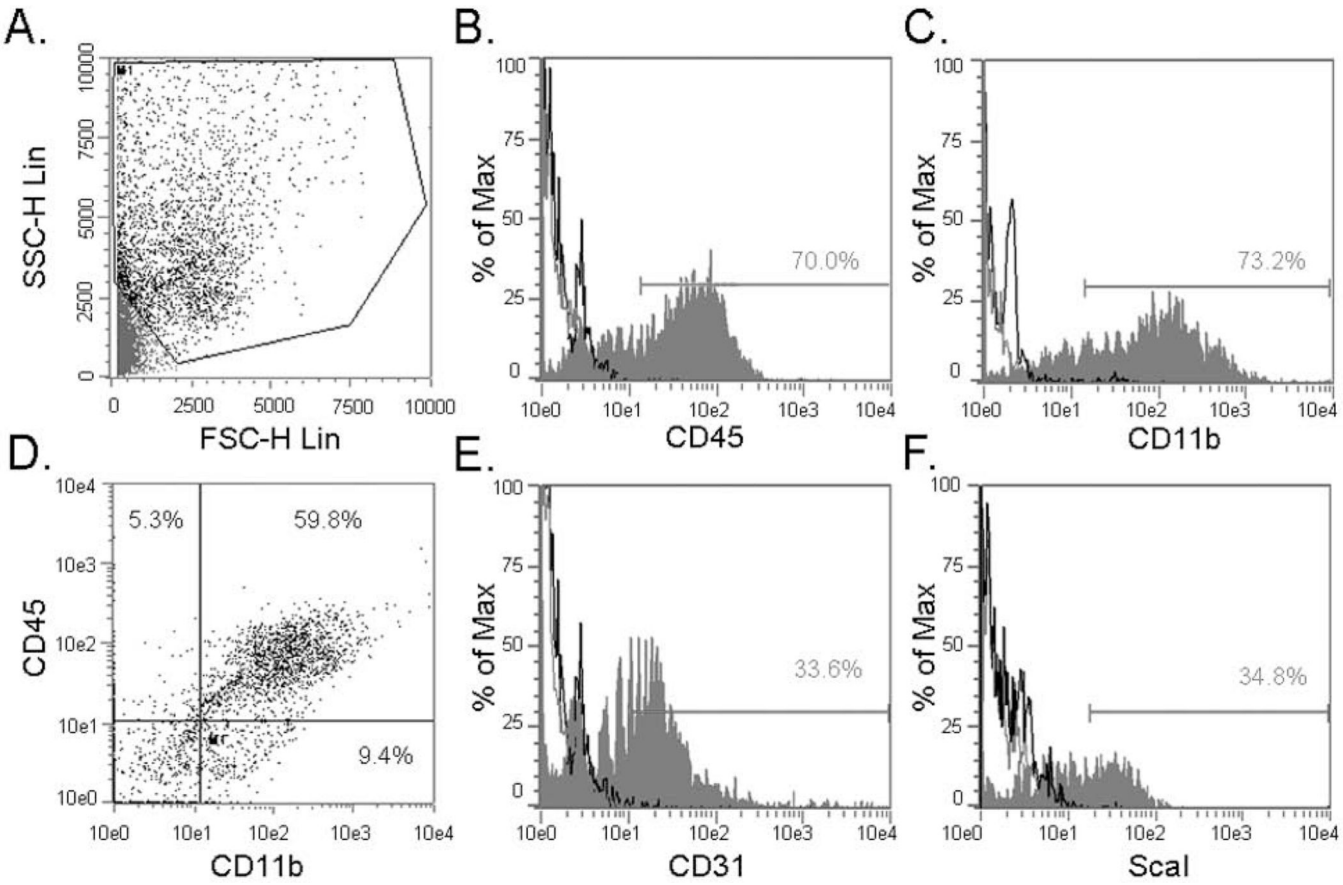

Figure 2.

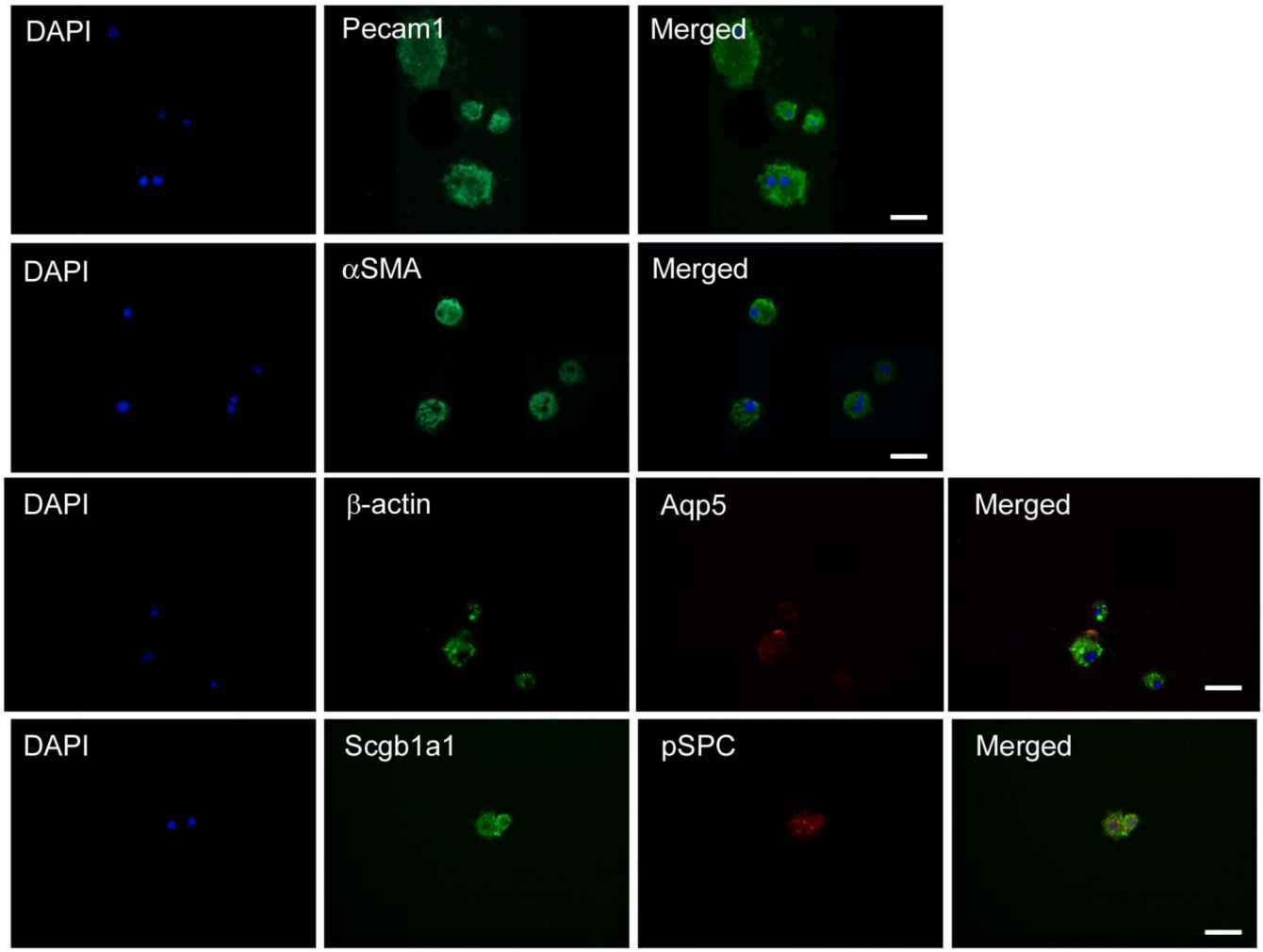

Figure 3.

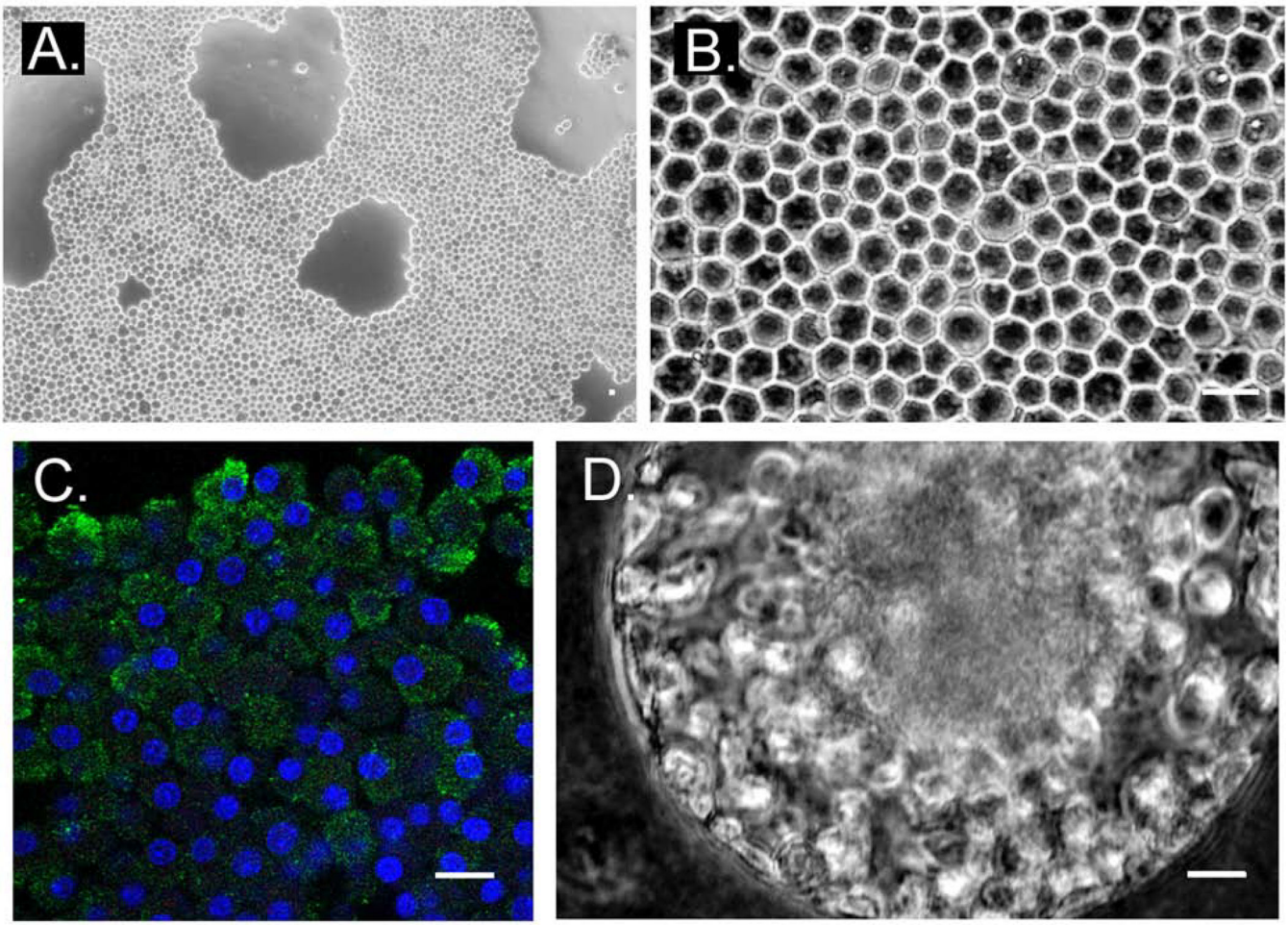

Figure 4.

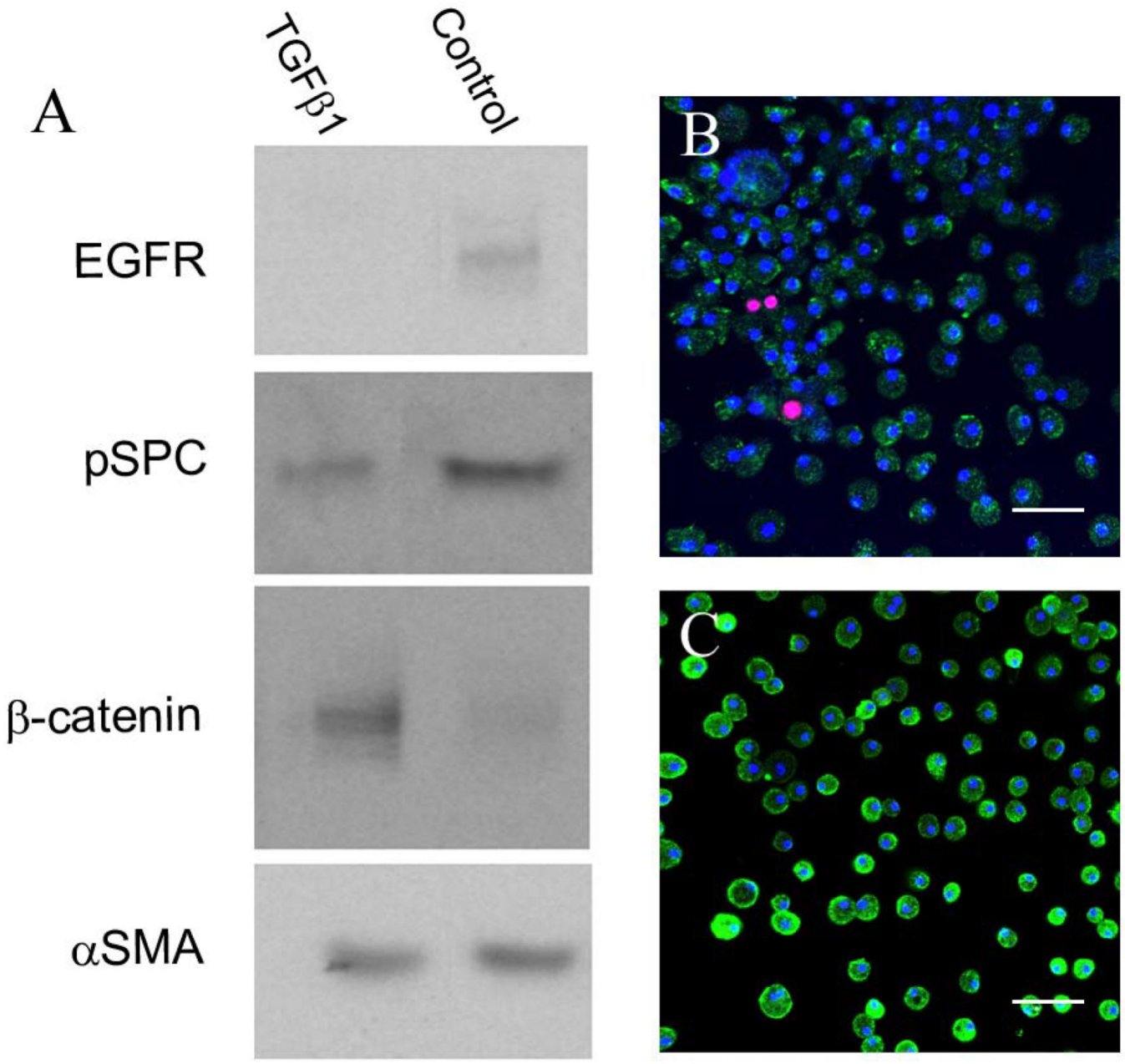

Figure 5.

J Tissue Eng Regen Med. Author manuscript; available in PMC 2015 May 18.

Table 1

Multilineage composition of the AIC population

Data illustrate relative qRT-PCR gene transcript levels of lung and AIC subsets.

Cell fraction	Cebpa	Scgb1a1	Sftpb	pSPC	Aqp5	Pecam1
Mouse lung	1.26 ± 0.14	1.02 ± 0.21	1.21 ± 0.24	1.24 ± 0.38	1.41 ± 0.24	1.12±0.21
AIC	1.34 ± 0.07	1.53 ± 0.13	1.60 ± 0.15	1.68 ± 0.19	1.53 ± 0.21	1.26 ± 0.19
CD45/CD11b	1.33 ± 0.06	1.48 ± 0.11	1.51 ± 0.15	1.63 ± 0.1 A*	1.59 ± 0.14^	1.04 ± 0.10*A**
CD45/Sca-1	1.35 ± 0.10 1*	1.61 ± 0.07*A*;1****	1.60 ± 0.17	1.84 ± 0.14 #*A*;1**	1.70 ± 0.15	1.17 ± 0.10*A;1*****
CD11b/Sca-1	1.35 ± 0.05	1.58 ± 0.03*1***	1.67 ± 0.33	ND	1.76 ± 0.07&*A;1***	1.12 ± 0.13*A**

Values represent mean ± standard deviation normalized to GAPDH RNA control (n≥5). Mouse lung, snap-frozen tissue; AIC, AIC population at 7-day in culture; and day 7 AICs sorted for: CD45/CD11b, CD45/Sca-1, and CD11b/Sca-1 double positive subsets.

Expression of pSPC and Aqp5 transcripts in the sorted populations was variable and either not detected (ND) or found in ^37% (10/27), #45% (9/20), or &56% (5/9) of the experiments with descriptive statistics limited to positive samples.

A Statistically significant against the AIC; and/or

1 the CD45/CD11b population with p-values of * p< 0.05; **p<0.01; or ***p<0.001.

Table 2

AIC population dynamics in culture

Cells were collected, prepared, labeled, and acquired by flow cytometry at days 6 and 21 ($n \geq 4$).

	Day 6 %AIC (Cells ×10^6)	Day 21 %AIC (Cells ×10^6)
CD45	58.59 ± 5.56 (3.12 ± 0.29)	88.33 ± 4.06* (5.08 ± 0.23)
CD11b	59.69 ± 3.75 (3.18 ± 0.20)	76.49 ± 4.94 (4.41 ± 0.28)
cKit	55.76 ± 3.32 (2.98 ± 0.18)	4.59 ± 4.79*** (0.26 ± 0.28)
Pecam1	37.13± 11.30 (1.98 ± 0.60)	18.30 ± 7.13 (1.05 ± 0.41)
EGFR	12.20 ± 4.02 (0.65 ± 0.21)	13.53 ± 2.54 (0.78 ± 0.15)

Upper values show percentage of cells in the AIC population (average ± SEM). Lower values (shown in parentheses) reflect the calculated number of antigen-presenting cells per lung per day. CD11b is produced in monocytes and cKit is produced in mast and hematopoietic stem cells. Pecam1 is found in endothelial cells and the epidermal growth factor receptor (EGFR) is expressed in epithelial cells. The percentage (and number) of $CD45^+$, a pan-hematopoietic marker, cells significantly increased, while that of cKit expressing cells significantly declined with time in culture.

* $p = 0.05$;

*** $p < 0.001$ by F test.